Light absorption and scattering of 40–170 nm gold nanoparticles on glass substrates

Ranveig Flatabø, Vårin R. A. Holm, Håkon Eidsvåg, Bodil Holst, and Martin M. Greve[a)]
Department of Physics and Technology, University of Bergen, Allégaten 55, 5007 Bergen, Norway

(Received 4 July 2017; accepted 31 October 2017; published 21 November 2017)

The localized surface plasmon resonance (LSPR) effect in metal nanoparticles is important for many applications ranging from detectors and sensors to photovoltaic devices. The LSPR wavelength is sensitive to the shape, size, surface condition, and surrounding environment. Therefore, it is important to compare the optical properties of metal nanoparticles of nominally similar dimensions and external conditions, but fabricated with different techniques. Here, a systematic study of the optical properties of large, periodic arrays (3×3 mm) of cylindrical, gold nanoparticles with diameters ranging from 39 ± 4 nm to 167 ± 5 nm and a height of 25 ± 1 nm is presented. The large arrays allow us to investigate the optical properties using an integrating sphere setup collecting the light scattered and absorbed by the nanoparticles. To the best of our knowledge, such a setup has not been used previously for electron beam lithography (EBL) fabricated samples mainly due the large sample area required. The authors compare our results with relevant literature and find a good agreement, which confirms the expected reproducibility of EBL. Further, the authors compare our absorption and scattering measurements with previous absorption and scattering measurements on large arrays of gold nanoparticles prepared on glass using hole-mask colloidal lithography. Finally, a comparison with simulations using a finite difference time domain software package (Lumerical, Inc.) is presented. The simulation results matches well with experimental results and are also supporting and detailing our comparison with published literature. The authors find a good agreement between the two fabrication methods. The small deviations found can be contributed to differences in the particle size and density distributions. *Published by the AVS.* https://doi.org/10.1116/1.4994113

I. INTRODUCTION

Over the last years, several studies have been carried out investigating the optical properties of metal nanoparticles.[1–3] The localized surface plasmon resonance (LSPR) effect can potentially be used in several applications ranging from detectors, sensors, and drugs to photovoltaic devices.[4–6] Several studies have revealed how minute differences in shape, surface condition, and surrounding environment can have a significant effect on the LSPR wavelength.[7,8] In this paper, we focus on gold nanoparticles prepared directly on glass substrates using lithography techniques.[9–11] The advantage of lithography is that the size of the nanoparticles, as well as the spacing between them on the substrate can be well controlled. The disadvantage, particularly for electron beam lithography (EBL), is that it takes a long time to prepare large samples.[12] For this reason, earlier studies of EBL fabricated metal nanoparticles have mostly been carried out on small ensembles, and the optical properties have mainly been investigated using optical microscopes in combination with a spectrophotometer, allowing the nanoparticle light extinction to be investigated. Such an investigation of gold nanoparticles can be found in Refs. 9–11 and 13–18. Furthermore, light scattered by metal nanoparticles can be studied using dark field spectroscopy, which in addition can allow changes in the polarization of light to be studied.[2,19–21]

Extinction is a measure for the light absorbed and scattered by the nanoparticles. For small particle sizes, absorption is dominant and the extinction spectrum thus gives a direct measure of the LSPR wavelength. However, for nanoparticle sizes above approximately 50 nm, light scattering becomes increasingly important. Hence, for nanoparticles larger than 50 nm, all the scattered light needs to be collected in order to obtain a proper absorption spectrum, that is, the LSPR wavelength. This has been done for gold nanoparticle arrays prepared on glass using hole-mask colloidal lithography (HCL),[11] but to our knowledge, up till now, not for EBL prepared arrays.

II. EXPERIMENT

A. Sample preparation

Large area arrays (3×3 mm) of gold nanoparticles were fabricated on glass using EBL (Raith e_Line). Gold is known to adhere quite badly on glass (dielectric materials). However, the use of an intermediate adhesive layer, such as commonly used thin film of titanium,[22] was not desirable as this affects the optical properties. We found that the nanoparticles stuck reasonably well to borosilicate glass microscope coverslips (Thermo Scientific). In order to realize the range of different nanoparticle sizes, a bilayer resist scheme was used. The bilayer scheme used in this work is carried out by first spin coating approximately 70 nm film of a high sensitivity PMMA resist [PMMA 495 K (Microchem 495 K PMMA)]. This was then baked at 175 °C for 5 min, followed

a)Electronic mail: martin.greve@uib.no

by another spin coating of a lower sensitivity PMMA resist [PMMA 950 K (Allresist AR-P 672.02)], and the sample was again baked at 175 °C for another 5 min. The higher sensitivity resist ensures a good undercut for the subsequent lift off, and the lower sensitivity a good EBL resolution. A charge dissipating 3 ± 1 nm film of chrome was deposited on top of the resist using electron beam evaporation (Temescal FC-2000). The resists were exposed using a 20 kV acceleration voltage, 20 μm aperture, a working distance of 10.5 mm, and an area dose of 120 μC/cm^2. For nanoparticle diameters of 72 nm and below, a dot exposure was used instead of area elements, using a dot dose of 0.0045 pC. The chrome layer was removed in a chrome wet etch, and the PMMA was developed by submerging the sample in a standard resist developer (Allresist AR 600-56) for 2 min. A 25 ± 1 nm gold film was deposited by means of electron beam evaporation (measured using an ellipsometer (Filmetrics F10-RT). Finally, the PMMA and the excess gold film was removed in a lift of step, by submerging the samples in *N*-methyl-2-pyrrolidone heated to 80 °C for about 30 min. The arrays were carefully rinsed using 2-propanol, and subsequently dried with compressed nitrogen gas. Nanoparticle arrays with diameters between 39 ± 4 and 167 ± 5 nm and a height of 25 ± 1 nm were fabricated. The arrays were arranged in a simple cubic pattern with lattice parameters greater than three times the nanoparticle diameter. A total of six arrays were prepared. Note that the SEM images were obtained without coating the samples with a conductive layer. Imaging of metal structures on insulating substrates can lead to distortion of the measured dimensions through substrate charging; however, by using specific settings in the SEM, true dimensions can be measured and relatively good still images acquired. This is discussed extensively in Ref. 23. The reason for not to coat the samples for SEM imaging is that the additional coating clearly would affect the optical properties, and it is desirable to keep the samples for future reference. To ensure reliable measurements, the SEM image settings used were a 2.5 kV beam with 10 μm aperture and a working distance of 10 mm.[23] Table I shows the sample overview presenting the actual versus targeted diameters, based on image analysis of on average 20 nanoparticles from each array. Note that the shape of the 167 nm nanoparticle (sample I) is found to be slightly elliptical, which causes the error bars to become relatively large.

B. Optical measurement setup

The large nanoparticle arrays fabricated in this work enabled us to investigate the optical properties using an integrating sphere setup (Ocean Optics ISP-50-8) and an extinction measurement setup (see Fig. 1). In the integrating sphere setup, the reflected and forward scattered light can be measured simultaneously over large solid angles. It consists of two spheres, with the sample sandwiched in between the spheres. The sphere walls are coated with a material yielding a Lambertian surface, having a reflectivity of greater than 98% for all wavelengths of interest. Light is incident upon the sample at 8°, and the uniform illumination (radiant flux) of the integrating spheres is measured using an optical fiber attached to the measurement port, yielding the spatial light– sample interaction. It should be noted that phase and polarization information is lost. To separately measure the sample extinction, a different setup using optical fibers for illuminating and collecting the signal is used [see Fig. 1(b)]. Since the incident angle of the light in the integrating spheres is not perpendicular to the sample surface, the sample is tilted 8° in the extinction setup so that the different measurements can be compared.

TABLE I. Sample overview.

Sample	Nanoparticle size (nm)	Interparticle distance (nm)	Nanoparticle height (nm)	Surface coverage
A	39 ± 4	145 ± 2	25 ± 1	0.0568
C	72 ± 4	290 ± 2	25 ± 1	0.0559
E	80 ± 10	400 ± 2	25 ± 1	0.0314
G	125 ± 2	450 ± 2	25 ± 1	0.0606
I	167 ± 15	600 ± 2	25 ± 1	0.0608

The extinction coefficient (E) can be written as

$$E = S + A, \tag{1}$$

where S is the scattering coefficient and A the absorption coefficient. The light reflected by the nanoparticles is detected in the reflection sphere, and we refer to this as S_R. In the transmission sphere, both the forward scattered light

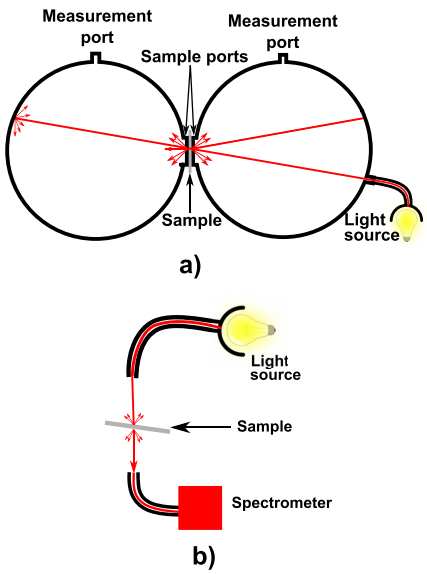

FIG. 1. (Color online) (a) Schematic illustration of the integrating sphere setup. The sample is sandwiched between the two spheres, and light is guided to, and collected from, the spheres using optical fibers. The acceptance angle of the measurement fiber is so low that there is no direct line of sight between the incident light and any first order reflections from the sphere walls. (b) Schematic illustration of the extinction measurement setup, used only for measuring the extinction separately. Note that the sample is tilted 8° relative to the incident beam, so that the different measurements can be compared.

and the directly transmitted (or extinct) light is detected. The forward scattered light by the nanoparticles, which we abbreviate S_T, can be calculated via the relation

$$S_T = E - T, \tag{2}$$

where T is the total amount of light detected in the transmission sphere. The light scattered by the sample in all spatial directions is then

$$S = S_R + S_T. \tag{3}$$

Combining this with Eq. (1) the light absorbed by the sample can be found. In order to extract the optical properties of the nanoparticles, the substrate (glass) was measured in the same manner, and its contribution subtracted. It should be noted that we discovered a notably variation in the optical properties between the individual substrates used for the nanoparticles arrays. Therefore, we found that it was crucial to measure the optical properties of the substrate close to the nanoparticle array on the same sample to achieve reliable results.

With the known nanoparticle absorption (A_{NP}) and (S_{NP}) constituting the overall nanoparticle scattering, the measurements are normalized to the real nanoparticle cross section, known as the scattering (Q_{sca}) and absorption efficiency (Q_{abs}),[24]

$$Q_{sca} = S_{NP}/(N\pi(d/2)^2), \tag{4}$$

$$Q_{abs} = A_{NP}/(N\pi(d/2)^2), \tag{5}$$

where N is the normalized unit cell coverage, and $\pi(d/2)^2$ is the cross-sectional area of a cylindrical shaped nanoparticle, where d is the nanoparticle diameter.

The center wavelength of the extinction peak is also important for comparison with the published literature (see Fig. 3).

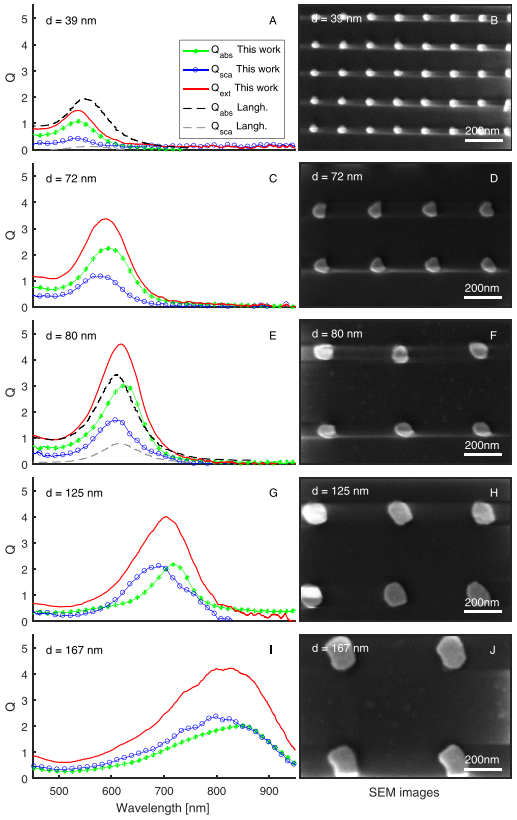

FIG. 2. (Color online) Measured extinction (red, solid line), absorption (green, asterisk marker) and scattering (blue, ring marker) efficiency of our fabricated arrays. For (a) and (e), measured values of gold nanoparticle arrays presented by Langhammer *et al.* (Ref. 11) is included for arrays of 38 and 76 nm (dashed black and gray lines). Those results are of relevance as the method of fabrication (HCL) is different, but the samples are also investigated using integrating spheres, measuring the scattering and absorption efficiency. In the right column, SEM images of a few of the nanoparticles from each sample are shown. Note that the images are captured under charging conditions, as we deliberately did not coat the samples.

C. Modeling

We used the FINITE DIFFERENCE TIME DOMAIN (FDTD) software package (Lumerical, Inc.) to model the absorption and scattering spectra. A $1200 \times 1200 \times 1200\,\text{nm}^3$ FDTD simulation space with perfectly matched layer (PML) boundaries is used as the simulation space. A 20, 25, or 50 nm high gold disk is placed on a SiO_2 glass substrate in the center of the space. The diameter of the disk is varied between 20 and 200 nm. A light source injects a plane wave from 25 nm above the disk and subtracted 25 nm after it has passed the disk, leaving only scattered light past these points. A scattering monitor is placed at 30 nm above and below the nanoparticle to study the near-field of the particle. The monitor is 270 nm wide to completely surround the nanoparticle. Similarly, an absorption monitor is placed between the light source and the nanoparticle, detecting incident light on one side and transmitted and scattered light on the other, giving

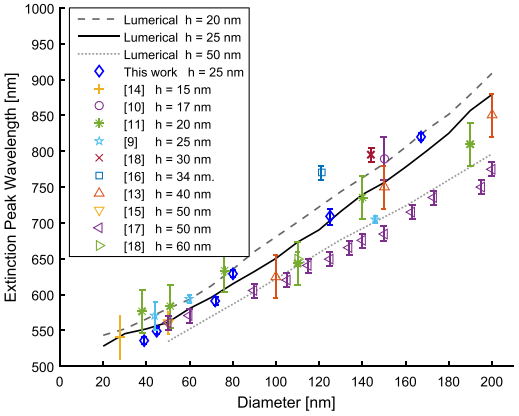

FIG. 3. (Color online) LSPR extinction peak resonance wavelength plotted against the gold nanoparticle diameter, for this experimental and theoretical work and several other sources in the literature (Refs. 11 and 13–18).

the net difference, i.e., the absorption. Reflection and transmission of the bare substrate is assumed to be negligible. The mesh size is set to be 3 nm for diameters 200–160 nm, 2 nm for the 150–90 nm diameter, 1.5 nm for 80 nm–60 nm, and 1 nm for 50–20 nm. The different mesh sizes are selected for efficient simulation time with sufficient accuracy. A field time monitor is included to record the time evolution of the electromagnetic fields, to ensure that the fields have enough time to decay before the maximum simulation time is reached. The light source covers wavelengths from 400– to 1050 nm. As no information about polarization can be extracted from the integrating sphere setup, the polarization is not considered in the simulation.

III. RESULTS AND DISCUSSION

A. Optical properties

In Figs. 2(a), 2(c), 2(e), 2(g), and 2(l), the measured extinction, scattering, and absorption of the nanoparticle arrays are presented. The contribution from the glass substrate has been removed by subtracting the corresponding spectrum measured on the same glass substrate, close to the nanoparticles (see Sec. II B). The nanoparticle extinction, scattering, and absorption efficiency spectra (Q_{ext}, Q_{sca}, and Q_{abs}) are plotted. For each fabricated array, a high magnification SEM image is included. All SEM images are acquired using the same magnification so that the area coverage and nanoparticle spacing can be easily evaluated. Note that the somewhat poor SEM image quality is due to the insulating nature of the substrate resulting in charging effects seen as brightness/contrast variation across the sample. In addition, data from the HCL gold nanoparticle samples presented by Langhammer *et al.*,[11] also studied using an integrating sphere, are included for comparison where a sufficient overlap in nanoparticle sizes are found. We will refer to this paper simply as Langhammer for the rest of this paper. The two samples of Langhammer having a diameter of 38 and 76 nm were sufficiently close to our 39 and 80 nm nanoparticle diameters. These four samples are presented together in Figs. 2(a) and 2(e). Comparing the results, it is seen that for the 38 nm nanoparticles, Langhammer measures an absorption efficiency which has a broader and slightly red-shifted center wavelength. Langhammer states that the standard deviation of the size distribution for the 38 nm nanoparticles is 20%, much larger than in our experiment, and hence the broader peak. The slight redshift can be explained as a coupling between some of the particles, which will give a shift toward higher wavelengths: To confirm this, we performed an image analysis of the SEM image provided by Langhammer (using the software ImageJ). We found an average particle diameter of 39 nm, a minimum size of 19 nm, and a maximum size of 54 nm. This is in good agreement with what Langhammer states. Based on the area coverage, the average distance between nanoparticles is 115 nm. This is about three times the particle diameter, sufficient to avoid near-field (interparticle) coupling. However, it should be noted that our image analysis revealed that some particles are only 80 nm apart, and for such closely spaced particles, interparticle coupling is expected.[10] The scattering efficiency of Langhammer similarly shows a redshift and is found to have a lower amplitude, as expected for coupled particles.[28]

For our 80 nm nanoparticles, we find that the peak is slightly narrower and shifted toward longer wavelengths compared to the 76 nm sample of Langhammer. This is considered a good agreement considering our slightly larger particle sizes, and that Langhammer uses a particle height of 20 nm compared to our height of 25 nm. The standard deviation of the size distribution for the 76 nm sample is stated to be less than 5%, which is slightly smaller than ours. Langhammer does not provide any SEM images of the larger gold nanoparticle samples, so we cannot check for any near-field coupling effects. However, the experiments do not indicate any. The scattering efficiency shows similar trends, but for our array, the scattering amplitude is higher. Also, we see slightly more scattering at shorter wavelengths.

Focusing on our samples 39, 72, and 80 nm [see Figs. 2(a), 2(c), 2(e)], it is found that the light absorption dominates over scattering. This is expected for particles smaller than 100 nm.[24] The minor rise in absorption efficiency at shorter wavelengths is attributed to interband transitions. Also, it can be seen that the scattering efficiency has some contribution at shorter wavelengths. This is somewhat unexpected as interband transition should only lead to absorption of light. Similar effects can be seen for Langhammer. It is however less pronounced which could be due to a lower signal. We speculate that the particles exhibit an increase scattering efficiency at shorter wavelengths, causing this effect. For the 125 and 167 nm nanoparticle samples [Figs. 2(g) and 2(i)], it is worth noting that the extinction efficiency is seen to broaden for the increasing particle size. The extinction peak wavelength is seen to red shift with increasing particle size as expected for a single particle.[17,25] The scattering efficiency can be seen to increase and finally becomes dominating. In an array of nanoparticles, near-field and far-field coupling must also be considered to contribute to the optical properties. The interparticle distance is equal to or greater than three times the particle diameter in all of the fabricated samples, which is sufficient to avoid near-field coupling.[10] However, as the particle diameter increases, so does the interparticle distances. For the increasing interparticle distances, far-field coupling will become increasingly evident. For such arrays, the scattered light of the nanoparticles will give rise to additional diffraction effects.[26,27] This far-field coupling has been shown to alter the measured extinction spectra by shifting the center peak position and its amplitude as a function of the nanoparticle periodicity.[27] For the 125 nm nanoparticle array, this is first of all seen as a broadening of the extinction efficiency. Measuring the nanoparticle absorption and scattering efficiency, this reveals, somewhat surprisingly, that the center wavelengths of the two does not coincide. We try to explain this as follows: first, we consider the absorption spectrum to mainly be a measure of the particle properties and near-field effects, whereas the scattering spectrum is affected by the far-field. The absorption spectrum will therefore exhibit single-particle-like optical properties, for these noninteracting nanoparticle arrays. The scattering spectrum on the other hand will contain the single

particle properties, strongly influenced by any far-field effects. This is evident as a blue shifted and broadened scattering spectrum, with respect to the absorption spectrum. Studying the extinction spectrum compares well with the findings of Lamprecht *et al.*[27] for a interparticle spacing of 450 nm.

Bearing the 125 nm sample in mind, one would expect a similar result for the 167 nm nanoparticle array, which turns out not to be the case. The center wavelength of the scattering and absorption spectra does not coincide. The scattering exhibits the expected broad shape, but the absorption is found to be much broader than expected from the above argument. This can likely be explained by the elliptical shape of the 167 nm nanoparticles which will give rise to the much broader absorption peak. Considering the extinction spectra, we can again see that an interparticle distance of about 600 nm should lead to a significant broadening of the LSPR due to far-field interaction.

Overall, the highest scattering and absorption efficiency is found for the 80 nm sample. For the largest diameters [125 and 167 nm, see Figs. 2(g) and 2(i)], both the scattering and absorption efficiency are seen to increasingly broaden. This is caused by the accumulative effect of (1) increasing particle diameter and size distribution and (2) far-field coupling, as discussed earlier.

B. Extinction peaks

As mentioned earlier, most investigations on lithography fabricated metal nanoparticles have been focused on measuring the extinction spectra to determine the center position of the extinction peak (the maximum position of the spectrum). In Fig. 3, we show the extinction peaks obtained in this work together with results previously published in the literature.[11,13–18] In addition, we have included new simulation results. The simulated peak position for gold nanoparticles ranging in diameters from 20 to 200 nm is presented for three nanoparticle heights, 20, 25, and 50 nm. Good agreement can be seen for all experimental data included in this work and our simulated results. We find a near linear relationship between the nanoparticle diameter and the LSPR wavelength for the fixed nanoparticle height, where the slope is depending on the nanoparticle height.

IV. SUMMARY AND CONCLUSION

In summary, we have fabricated large arrays of gold nanoparticles by means of EBL with diameters in the range 39 ± 4 to 167 ± 15 nm and interparticle distances equal to or greater than three times the particle diameter. The optical properties of the arrays were investigated using an integrating sphere setup, which allows us to measure the light absorption and scattering. We compare a set of samples with hole mask colloidal lithography fabricated nanoparticle samples where the optical properties were also studied using integrating spheres. We find a good agreement.

For the larger nanoparticle diameters (125 and 167 nm), the scattered light gives rise to additional diffraction effects due to the increased interparticle distances (grating period). These effects alter the measured optical properties significantly. However, measuring the absorption and scattering allow us to navigate these unexpected results. We can distinguish far-field effect from the absorption, which shows the expected optical properties of a noninteracting single nanoparticle. Using ordered arrays will give rise to such effects in the far-field, which can be avoided by using nonordered arrays achieved by, e.g., HCL.

Finally, we present extinction measurements as a function of the nanoparticle diameter, which we compare to results on EBL and HCL fabricated nanoparticle arrays already published in the literature. These plots are supported by simulations, which agree well with the experimental results.

ACKNOWLEDGMENT

Ranveig Flatabø gratefully acknowledges the support from the Bergen Research Foundation. The authors also thank the reviewers for their fruitful feedback.

[1]C. L. Haynes and R. P. Van Duyne, J. Phys. Chem. B **105**, 5599 (2001).
[2]C. L. Nehl, H. Liao, and J. H. Hafner, Nano Lett. **6**, 683 (2006).
[3]O. Nicoletti, F. Pena, R. K. Leary, D. J. Holland, C. Ducati, and P. A. Midgley, Nature **502**, 80 (2013).
[4]M. W. Knight, H. Sobhani, P. Nordlander, and N. J. Halas, Science **332**, 702 (2011).
[5]K. M. Mayer and J. H. Hafner, Chem. Rev. **111**, 3828 (2011).
[6]M. Tu, T. Sun, and K. Grattan, Sens. Actuator, B **164**, 43 (2012).
[7]V. R. A. Holm, M. M. Greve, and B. Holst, J. Vac. Sci. Technol., B **34**, 06K501 (2016).
[8]K. A. Willets and R. P. V. Duyne, Annu. Rev. Phys. Chem. **58**, 267 (2007).
[9]M. M. Greve, T. O. Håvardstun, and B. Holst, J. Vac. Sci. Technol., B **31**, 06F410 (2013).
[10]W. Rechberger, A. Hohenau, A. Leitner, J. Krenn, B. Lamprecht, and F. Aussenegg, Opt. Commun. **220**, 137 (2003).
[11]C. Langhammer, B. Kasemo, and I. Zorić, J. Chem. Phys. **126**, 194702 (2007).
[12]M. M. Greve and B. Holst, J. Vac. Sci. Technol., B **31**, 043202 (2013).
[13]T. Temple and D. Bagnall, J. Appl. Phys. **109**, 084343 (2011).
[14]G. Niklasson and H. Craighead, Thin Solid Films **125**, 165 (1985).
[15]X. Wang, P. Gogol, E. Cambril, and B. Palpant, J. Phys. Chem. C **116**, 24741 (2012).
[16]G. Bi, L. Wang, C. Cai, K. Ueno, H. Misawa, and J. Qiu, J. Mod. Opt. **61**, 1231 (2014).
[17]J. Grand, P.-M. Adam, A.-S. Grimault, A. Vial, M. Lamy de la Chapelle, J.-L. Bijeon, S. Kostcheev, and P. Royer, Plasmonics **1**, 135 (2006).
[18]N. Félidj, J. Aubard, G. Lévi, J. R. Krenn, M. Salerno, G. Schider, B. Lamprecht, A. Leitner, and F. R. Aussenegg, Phys. Rev. B **65**, 075419 (2002).
[19]E. Babich, S. Scherbak, F. Heisler, S. Chervinskii, A. Samusev, and A. Lipovskii, J. Phys.: Conf. Ser. **769**, 012040 (2016).
[20]T. Hoang, G. Akselrod, C. Argyropoulos, J. Huang, D. Smith, and M. Mikkelsen, Nat. Commun. **6**, 1 (2015).
[21]B. M. Reinhard, M. Siu, H. Agarwal, A. P. Alivisatos, and J. Liphardt, Nano Lett. **5**, 2246 (2005).
[22]B. Lahiri, R. Dylewicz, R. M. D. L. Rue, and N. P. Johnson, Opt. Express **18**, 11202 (2010).
[23]R. Flatabø, A. Coste, and M. Greve, J. Microsc. **265**, 287 (2017).
[24]C. F. Bohren and D. R. Huffman, *Absorption and Scattering of Light by Small Particles* (Wiley-VCH, Germany, 2007).
[25]A. Moroz, J. Opt. Soc. Am., B **26**, 517 (2009).
[26]M. Meier, A. Wokaun, and P. Liao, J. Opt. Soc. Am., B **2**, 931 (1985).
[27]B. Lamprecht, G. Schider, R. Lechner, H. Ditlbacher, J. Krenn, A. Leitner, and F. Aussenegg, Phys. Rev. Lett. **84**, 4721 (2000).
[28]J. R. Kenn, A. Dereux, J. C. Weeber, E. Bourillot, Y. Lacroute, and J. P. Goudonnet, Phys. Rev. Lett. **82**, 2590 (1999).